Histol Histopathol (2013) 28: 353-364
DOI: 10.14670/HH-28.353

http://www.hh.um.es

Histology and Histopathology
Cellular and Molecular Biology

Levels of acyl-Coenzyme A synthetase 5 in urothelial cells and corresponding neoplasias reflect cellular differentiation

Nadine T. Gaisa[1*], Andrea Reinartz[1*], Ursula Schneider[1], Christina Klaus[1], Axel Heidenreich[2], Gerhard Jakse[2], Elke Kaemmerer[1,3], Barbara Mara Klinkhammer[4], Ruth Knuechel[1] and Nikolaus Gassler[1]

[1]Institute of Pathology, RWTH Aachen University, Aachen, Germany, [2]Department of Urology, University Hospital Aachen, Aachen, Germany, [3]Department of Paediatrics, University Hospital Aachen, Aachen, Germany and [4]Department of Internal Medicine II, Nephrology and Clinical Immunology, University Hospital Aachen, Aachen, Germany

*NTG and AR share first authorship

Summary. Metabolic components like fatty acids and acyl-Coenzyme A (acyl-CoA) thioesters have been implicated in the pathogenesis of various tumours. The activation of fatty acids to acyl-CoAs is catalysed by long chain acyl-CoA synthetases (ACSLs), and impairment of ACSL expression levels has been associated with tumourigenesis and progression. Since ACSLs have never been investigated in bladder tissues, the study aims to characterize ACSL expression and acyl-CoA synthesis in normal and neoplastic bladder tissues, as well as cell lines. ACSL isoforms 1, 3, 4 and 5 and synthesis of acyl-CoAs were analysed using qRT-PCR, western blot analysis, immunohistochemistry and lipid mass spectrometry.

In normal urothelium, expression of ACSL1, 3, 4 and 5, with highest levels of ACSL isoform 5 was found. However, ACSL5 expression was reduced in corresponding neoplastic tissues and urothelial cell lines depending on the grade of cellular differentiation. Anti-ACSL5 immunostainings showed expression in normal urothelium and a gradual loss of ACSL5 protein via pre-invasive lesions to invasive carcinomas. High expression of ACSL5 correlated with increased α-galactosidase activity and positive Uroplakin III staining in tumours. In contrast, synthesis of acyl-CoAs was enhanced in neoplastic bladder tissues compared to normal urothelium, and reflected an increase with respect to cellular differentiation. These results confirm an expression of ACSLs, especially isoform 5, in human urothelium, prove enzymatic/lipidomic changes in bladder cancer tissues, and suggest an involvement of ACSL5 in cellular maturation and/or senescence with possible effects onto induction of tumour formation or progression. Further work may identify responsible pathway alterations, and attempting to re-balance the metabolic equilibrium of the urothelium may offer a further opportunity for tumour treatment and prevention.

Key words: ACSL, ACSL5, Bladder, Urothelium, Cancer

Offprint requests to: Prof. Dr. Nikolaus Gassler (M.A.), Institute of Pathology RWTH Aachen, Pauwelsstrasse 30, 52074 Aachen. Germany. e-mail: ngassler@ukaachen.de

Introduction

Bladder cancer is the ninth most common cancer worldwide with more than 300 000 new cases per year (Ferlay et al., 2010). Due to advances in diagnostics and therapy it has shown increasing survival rates by time; i.e. in the United States of America (USA) the 5-year survival rate for all types of bladder cancer has risen about 10% between 1975-1977 and 2001-2007 (Howlader et al., 2011). Nevertheless, due to the course of the disease with multiple syn- or metachronous tumours bladder cancer patients have to undergo (life-) long surveillance regimes, which turn bladder cancer into the neoplasia with the highest costs per patient among all cancers with up to more than $200.000 per patient (Hong and Loughlin, 2008). Therefore not only improvements in diagnostics and therapy but also progress in understanding tumour biology with impact for translational research, is a main goal in bladder cancer science.

In the past years tremendous effort was put into the genetics of bladder cancer and several key genes were identified (reviewed in Wu, 2005). However, little is known about metabolic changes/imbalances and bladder cancer. So far only a few reports have investigated the effects of dietary fat exposure on urothelium (Bongiovanni et al., 2005) and fatty acid dependent modulations of proliferation or apoptosis (Cremonezzi et al., 2001, 2004; Zhang et al., 2010). More recently, mass spectrometry on canine urothelial tissue has shown differences in lipid and free fatty acid levels between tumour and normal tissue (Dill et al., 2009), and the expression of 15-lipoxygenase-1 (15-LO-1), a polyunsaturated fatty acid (PUFA)-metabolizing enzyme, was found to be altered in bladder cancer progression (Philips et al., 2008). Although acyl-Coenzyme A synthetase (acyl-CoA synthetase, ACSL), especially isoform 5 (ACSL5), was studied in other (tumour-)tissues and found deregulated in gliomas (Yamashita et al., 2000), intestinal tumours (Gassler et al., 2003, 2005a) and endometrium cancer (Gassler et al., 2005b), the expression of ACSL5 has not yet been evaluated in urothelium and bladder cancer.

ACSLs are key enzymes in the fatty acid metabolism, which convert free long-chain fatty acids and coenzyme A to acyl-CoA thioesters. The products of ACSLs serve as substrates for complex lipid biosynthesis and energy metabolism (Soupene and Kuypers, 2008), and may also be involved in transport processes or regulation processes via signalling molecules (Faergeman and Knudsen, 1997). So far in humans, five different isoforms of acyl-CoA synthetase with different biochemical characteristics and tissue distribution have been described. ACSL1, 3 and 4 have been located to the epithelia of trachea, mouth, liver, and skin (Mashek et al., 2004). ACSL6 was found in neural tissues and leucocytes (Mashek et al., 2004), and ACSL 5 is mainly expressed in intestinal epithelia (Yamashita et al., 2000; Gassler et al., 2004, 2007). Our workgroup has previously suggested that isoform 5 might be functionally involved in differentiation and senescence of enterocytes (Gassler et al., 2007), differentiation and stress response of keratinocytes (Gaisa et al., 2008) and apoptosis of hepatocytes (Reinartz et al., 2010).

In the present study, we analyzed the ribonucleic acid (RNA) expression of ACSL 1, 3, 4 and 5 in urothelial cell lines as well as matched normal urothelium and cancer tissues. ACSL isoform 5 showed the highest expression levels of all ACSL isoforms, therefore, we further evaluated isoform 5 at protein level. The combined results of the study demonstrate an expression of ACSL5 in normal human urothelium with highest levels in terminally differentiated superficial cells, and a gradual loss of ACSL5 expression with decreasing cellular differentiation in urothelial cancers. In contrast to the loss of ACSL5 expression, mass spectrometry of acyl-CoAs, the products of ACSLs, revealed an increase of acyl-CoA synthesis with decreasing cellular differentiation in urothelial carcinoma and human bladder cancer cell lines.

Materials and methods

Tissues and cell culture

Mechanically dissected snap frozen normal urothelial linings and tumour tissues (n=21) from cystectomy specimes with muscle invasive bladder cancer were used. Sampling of tissues was approved by the local ethics committee at Rheinisch-Westfälische Technische Hochschule (RWTH) Aachen University (Ethikkommission (EK) 122/04, 206/09). Diagnosis and dissection was controlled by haematoxylin and eosin (H&E) stainings of reference cryosections. Grading and staging of urothelial carcinoma was assessed according to the World Health Organization/International Society of Urological Pathology (WHO/ISUP) 2004 classification; alternatively the tree-tier 1973 WHO/ISUP classification was given (Mostofi et al., 1973; Lopez-Beltran et al., 2004). Cell culture experiments were performed by using Urotsa (Simian-virus 40 (SV 40) transfected immortalized cell line out of normal urothelium of the ureter) for normal urothelial conditions (Rossi et al., 2001). For transitional cell carcinoma equivalents RT4 (clinical stage T2, histological grade G1 (Rigby and Franks, 1970)), RT112 (clinical stage not recorded, histological G2 (Masters et al., 1986)) and J82 (clinical stage T3, histological grade G3 (Masters et al., 1986)) were used. According to the 2004 WHO/ISUP classification RT4 and RT112 were considered as well differentiated tumour cell lines (low grade) and J82 as a poorly differentiated tumour cell line (high grade). RT4 cells were cultured under standard conditions with McCoy's 5A medium (PAN Biotech GmbH, Aidenbach, Germany), L-glutamine-penicillin-streptomycin (LGPS) and 10% fetal calf serum. For culture of RT112, J82 and Urotsa RPMI 1640 medium (PAA Laboratories GmbH, Cölbe, Germany), LGPS and 10% fetal calf serum were used. Cells were harvested in trizol (TRI reagent, Sigma, Steinheim, Germany).

RNA and protein isolation

Dissected tissues and cultured cells were homogenized in TRI reagent (Sigma) using an Ultra Turrax homogenizer (IKA Labortechnik, Staufen, Germany). Simultaneous preparation of RNA and protein according to the phase separation method by Chomczynski (1993) was performed. Precipitated RNA was dissolved in distilled water/RNAsin (Promega, Mannheim, Germany). RNA concentration was measured with NanoDrop ND-1000 spectrophotometer (NanoDrop Technologies, Wilmington, USA). Protein concentrations were estimated using BioRad assay reagent (BioRad, München, Germany) and Laemmli's buffer was added to one fold final concentrations.

Reverse transcription and quantitative polymerase chain reaction (RT-PCR)

SuperScript III amplification system (Invitrogen, Karlsruhe, Germany) was used for oligo (dT) primed first-strand copy desoxy ribonucleic acid (cDNA) synthesis from total RNA. Control transcription of a commercially provided RNA or substitution of the enzyme reverse transcriptase by distilled water was performed. ACSL isoforms 1, 3, 4 and 5 were amplified by Real Time PCR using IQ 5 detection system (BioRad, München, Germany) and appropriate primer pairs, including cyclophilin, as a housekeeping transcript (Table 1). Amplifications were performed by iQ Sybr-green Supermix (BioRad, München, Germany) under the following conditions (33 cycles; annealing temperature 63°C). Amplicon integrity was further evaluated by agarose gels (2%) stained with ethidium bromide (Sigma). Analysis of RT-PCR data was either performed with Relative Expression Software Tool (REST©) 2008 (Pfaffl, 2001; Pfaffl et al., 2002) for pair wise comparisons, or according to the ΔΔct method (comparative cycle threshold method) if multiple comparisons were analysed (Fink et al., 1998). Relative mRNA levels of ACSL1, 3, 4 and 5 were calculated with respect to the house keeping gene cyclophilin.

Sodium dodecyl sulfate polyacrylamide gel electrophoresis (SDS-PAGE) and Western blot analysis

Proteins in Laemmli's buffer were resolved by one-dimensional SDS-PAGE (7.5% gels, 30 μg protein per lane) and blotted in a semidry manner to polyvinylidene difluoride (PVDF) Immobilon-P membranes (Millipore Corporation, Bedford, USA). Protein blotting was controlled by Coomassie staining of gels and membranes. For protein detection anti-human ACSL5 antibody, clone 5H8 (dilution 1:500, Abnova, Heidelberg, Germany) and anti-human beta-actin (dilution 1:1000, Sigma, Taufkirchen, Germany), secondary horseradish peroxidase-conjugated antibodies (dilution 1:10.000; Santa Cruz, Santa Cruz, USA) and enhanced chemiluminescence (ECL) substrate (Amersham Pharmacia Biotech, Little Chalfont, United Kingdom) were sequentially applied. Equal loading of protein was controlled by analysis of beta-actin levels in each sample. Mitochondrial isolations from HepG2 cells overexpressing ACSL5 were used as a positive control; in negative controls the primary antibody was omitted.

Immunostainings

Formalin-fixed paraffin-embedded tissue sections (2 μm) were dewaxed, pretreated with heat (microwave) induced antigen retrieval in pH 6 buffer and incubated with monoclonal mouse anti-ACSL5 antibody (1:400, Abnova) over night at 4°C in a moist chamber. Secondary antibody anti-mouse, biotinylated (1:200, DAKO, Hamburg, Germany) and ABC-detection kit (Vector, Burlingame, USA) with diaminobenzidine (DAB) (Vector) were applied according to the manufacturer's instructions. For immunofluorescence sections (4 μm) were incubated with KD7 antibody (cell culture supernatant, see Gassler et al., 2003) followed by a biotinylated goat anti-rat antibody (Jackson-ImmunoResearch, Baltimore, USA) and finally the appropriate Cyanine (Cy) 3-labelled Streptavidin (JacksonImmunoResearch, Baltimore, USA) antibody was applied and counterstained with 4',6-diamidino-2-phenylindole (DAPI) I (Abbott, Des Plaines, USA). In negative controls buffer or appropriate normal serum for primary incubation were used. Evaluation of immunofluorescence stainings was performed with a Nikon 80i fluorescence microscope (Nikon, Düsseldorf, Germany). For immunohistochemistry on paraffin tissue sections (2 μm) or sections from formalin-fixed, agarose embedded cell pellets (2 μm) heat induced antigen retrieval with DAKO PTLink and EnVision™ FLEX target retrieval solution low pH or high pH were used (DAKO). Primary antibodies mouse anti-Cytokeratin 20 (1:200, clone K280.8, DAKO), rabbit anti-p53 (1:50, clone 318-6-11, DAKO), mouse anti-Uroplakin III (1:10, clone AU1, progen, Heidelberg, Germany) and mouse anti-p16INK4A (1:400, clone JC8, Santa Cruz Biotechnology Inc., Heidelberg, Germany) and appropriate EnVision™ FLEX+ mouse or rabbit system secondary antibody were applied in an Autostainer Link 48 (DAKO). Staining results were analysed in a semiquantitative manner using the immunoreactive scoring (IRS; product of staining intensity and percentage of positively stained cells) of Remmele (Remmele and Stegner, 1987) adapted for cytoplasmatic/membranous staining.

Senescence-associated-ß-galactosidase (sa-ß-gal) enzymehistochemistry

Cryosections (10 μm) from frozen tissue or cell pellets as well as cell lines were analysed for senescence-associated-ß-galactosidase activity. Urotsa, RT4, RT112 and J82 were seeded onto chamber slides (LAB-TEK®II, Nalge Nunc International, Naperville,

Table 1. Summary of all primer sequences used for RT-PCR.

Primer	Sequence 5'-3'	Product size
ACSL 1F	CCA GAA GGG CTT CAA GAC TG	
ACSL 1R	GCC TCC TCT GGC TTG TCA AC	203 bp
ACSL 3F	CCC GCC ACC AAC TTA CTT TA	
ACSL 3R	GCC CCC AAA TAA CCA ATT CT	204 bp
ACSL 4F	GGT CTG TTT GCT TTG CTG A	
ACSL 4R	ACT CTG CCC TTC TCC CAA AT	256 bp
ACSL 5F	TTT TTG TAC ACG GGG AGA GC	
ACSL 5R	ACA GGC TGT CAA TTT GGG TC	321 bp
Cyclophilin F	CAT TTG CCA TGG ACA AGA TG	
Cyclophilin R	ACC CCA CCG TGT TCT TCG AC	300 bp

Illinois, USA) at a density of $1.5x10^3$ cells/cm^2 (RT4 $1x10^5$ cells/cm^2) and cultured until sub-confluency. Cells were washed in phosphate buffered saline (PBS) and fixed in 0.5% glutaraldehyde for 10 min. Cryo-sections were also fixed in 0.5% glutaraldehyde for 10 min. Tissue sections and cell slides were incubated for 8 h at 37°C with fresh staining solution containing 0.1% x-Gal-solution (5-bromo-4-chloro-3-indolyl ß-galactosidase; Sigma), 40 mM citric acid/sodium-phosphate pH 6.5 mM potassium ferrocyanide, 5 mM potassium ferricyanide, 150 mM NaCl and 2 mM $MgCl_2$. Cells were counterstained with eosin and mounted with Malinol (Waldeck GmbH&Co KG, Münster, Germany). Staining results were analysed in a semiquantitative manner using a modified scoring system of Remmele (Remmele and Stegner, 1987).

Acyl-CoA extraction and analysis by Liquid chromatography - tandem mass spectrometry (LC-MS/MS)

Tissue samples (20 mg) or cells ($0.5\text{-}2x10^7$) were homogenized in 200 μl Aqua bidest using the Ultra-Turrax (ICA Labortechnik, Stauffen, Germany) and transferred into 13x100 mm borosilicate tubes with a Teflon-lined cap (VWR, West Chester, PA, USA). The acyl-CoAs were extracted and prepared for liquid chromatography electrospray ionization-tandem mass spectrometry (LC ESI-MS/MS) as described previously (Haynes et al., 2008). After transfer of the suspension to the autoinjector vial for analysis, acyl-CoAs were separated by reverse phase LC using a Gemini 5u C18 110A 150x2.00 mm column at a flow rate of 0.2 ml/min and a binary solvent system. After sample injection, the column was equilibrated for 5 min with 100% Mobile phase A (85:15, H_2O: C_2H_3N, with 0.05% $N(CH_2CH_3)_3$) followed by a 14 min linear gradient to 50% Mobile phase B (10:90, H_2O: C_2H_3N, with 0.05% $N(CH_2CH_3)_3$) and an additional 1 min linear gradient to 100% Mobile phase B which was held for 5 min. Prior to the next run, the column was equilibrated with a 1 min linear gradient to 100% Mobile phase A which was maintained for 5 min. Acyl-CoAs were analyzed by LC ESI-MS/MS in positive ionization mode using an ABI 4000 QTrap mass spectrometer as previously described (Haynes et al., 2008). Quantitation was performed by MRM (multiple reaction monitoring) and comparison with the spiked internal standard (mixture of C15, C17, C23 and C25-CoA, each 100 pmol/ sample, Avanti Polar Lipids, Alabaster, Alabama, USA). Acyl-CoA quantities are

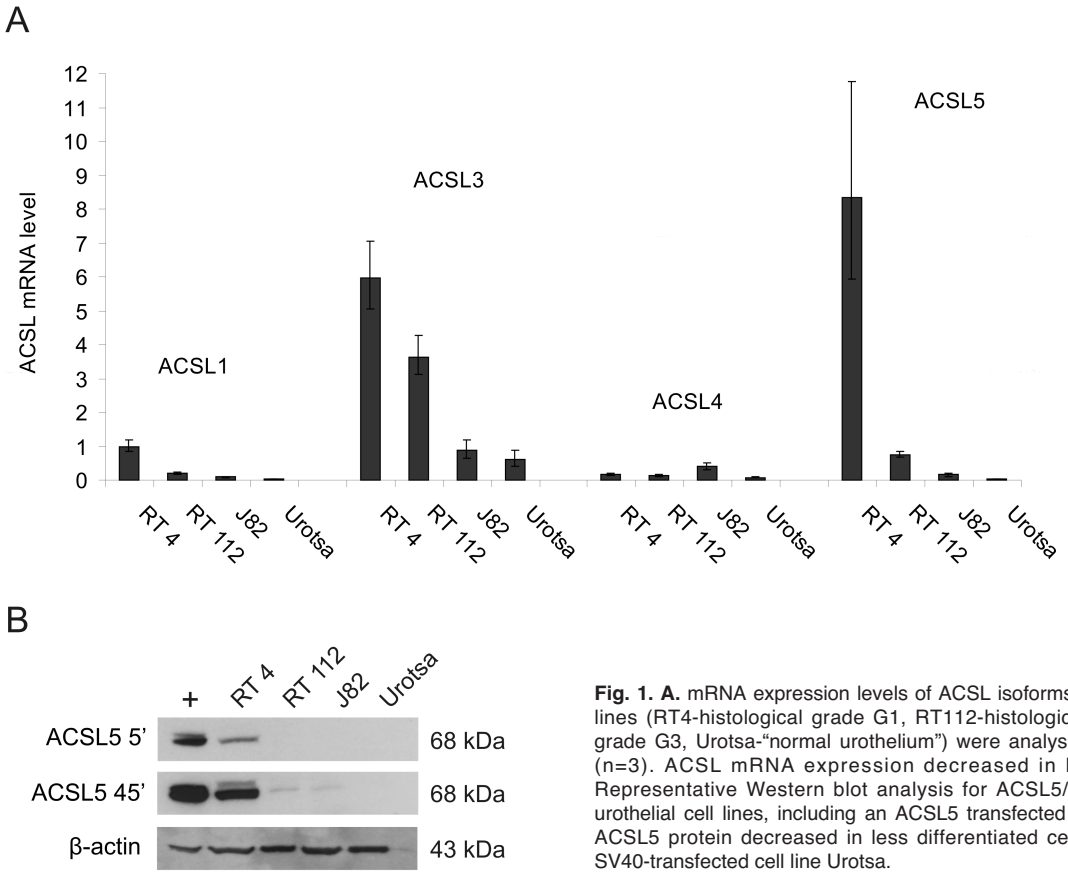

Fig. 1. A. mRNA expression levels of ACSL isoforms 1, 3, 4 and 5 in urothelial cell lines (RT4-histological grade G1, RT112-histological grade G2, J82-histological grade G3, Urotsa-"normal urothelium") were analysed using quantitative RT-PCR (n=3). ACSL mRNA expression decreased in less differentiated cells. **B.** Representative Western blot analysis for ACSL5/ß-actin protein expression in urothelial cell lines, including an ACSL5 transfected cell lysate as positive control. ACSL5 protein decreased in less differentiated cells and was not detectable in SV40-transfected cell line Urotsa.

expressed as pmol/ mg protein.

Statistical analysis

All experiments were reproduced at least three times. Representative Western blots and images of stained tissues or cells are shown. Unless otherwise stated, all results are presented as mean ± standard error, with n representing the number of tissue samples/ repetitions of each assay. The statistical significance of realtime PCR and acyl-CoA LC-MS/MS data was assessed with a two-tailed paired Student's t test; for immunohistochemistry/enzymehistochemistry data (Remmele-Score) the significance was assessed with a one-tailed unpaired Student's t test/Mann-Whitney U test. A value of $p<0.05$ was considered statistically significant.

Results

ACSL isoforms are expressed in urinary bladder (cancer) cell lines

Messenger RNA (mRNA) expression of ACSL5 and additionally isoforms 1, 3 and 4 was found in all human bladder cell lines (Fig. 1A). ACSL5 was the most abundant isoform found at expression levels (>8-fold higher than cyclophilin in RT4). In Urotsa the mRNA expression was generally lowest. ACSL5 showed a gradual decrease in mRNA-expression with histological dedifferentiation. The expression of ACSL5 was highest in cell lines that are considered as models for papillary-invasive bladder cancer low grade (G1 or G2); in J82 (solid, invasive G3 (high grade) transitional cell carcinoma stage T3) expression was lower.

Due to highest expression levels of ACSL5, confirmation aton protein level was done for ACSL5. Western blot analysis confirmed the results of RT-PCR; ACSL5 expression decreased with the differentiation grade of the cancer cell lines (RT4>RT112>J82), with the largest difference between RT4 and RT112 (Fig. 1B). ACSL5 protein expression in Urotsa was not detectable.

Expression of ACSLs is downregulated in bladder cancer

Also, in fresh frozen normal urothelium and tumour samples all ACSL isoforms could be detected by RT-PCR (Fig. 2A). Interestingly, ACSL isoform 5 was the

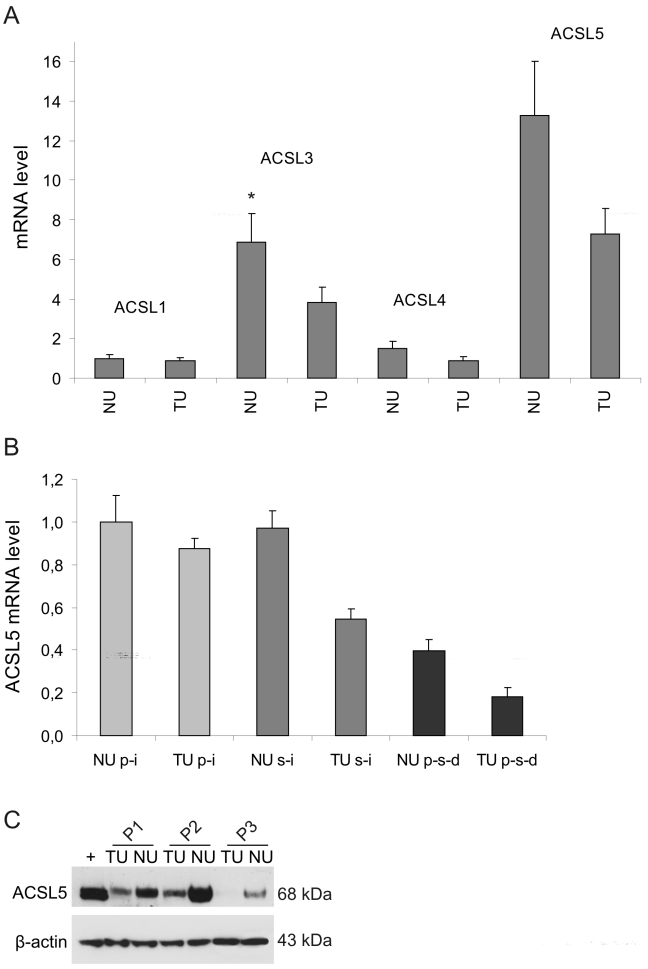

Fig. 2. A. mRNA expression levels of ACSL isoforms 1, 3, 4 and 5 in normal tissues (NU, n=18) compared with tumour tissues (TU, n=18). The highest mRNA expression level was found for ACSL5 in normal tissue. Differences in mRNA expression between normal urothelium and tumour with a downregulation in tumour tissue could be shown for ACSL 3, 4 and 5 (*p=0.001, p=0.06, p=0.095). **B.** Subdivision of tumour samples in papillary-invasive (p-i), solid-invasive (s-i) and partially squamous differentiated (p-s-d) types with respective normal urothelium as control revealed a decrease of ACSL5 mRNA expression only in solid-invasive and partially squamous differentiated, but not in papillary-invasive types (p>0.05). **C.** Representative Western blot analysis for ACSL5/ß-actin protein expression in normal and tumour urothelial tissues (n=14) including an ACSL5 transfected cell lysate as positive control. ACSL5 protein expression was decreased in tumour tissues when compared to normal tissues.

Table 2. Summary of significant (p<0.05) up- or downregulations of ACSL isoforms in tumour tissue normalized to matched normal urothelium of each patient.

	ACSL1	ACSL3	ACSL4	ACSL5
All significant regulations	61.1% (11/18)	61.1% (11/18)	50% (9/18)	88.89% (16/18)
Sign. upregulation in tumours	33.3% (6/18)	16.7% (3/18)	5.6% (1/18)	27.8% (5/18)
Sign. downregulation in tumours	27.8% (5/18)	44.4% (8/18)	44.4% (8/18)	61.1% (11/18)

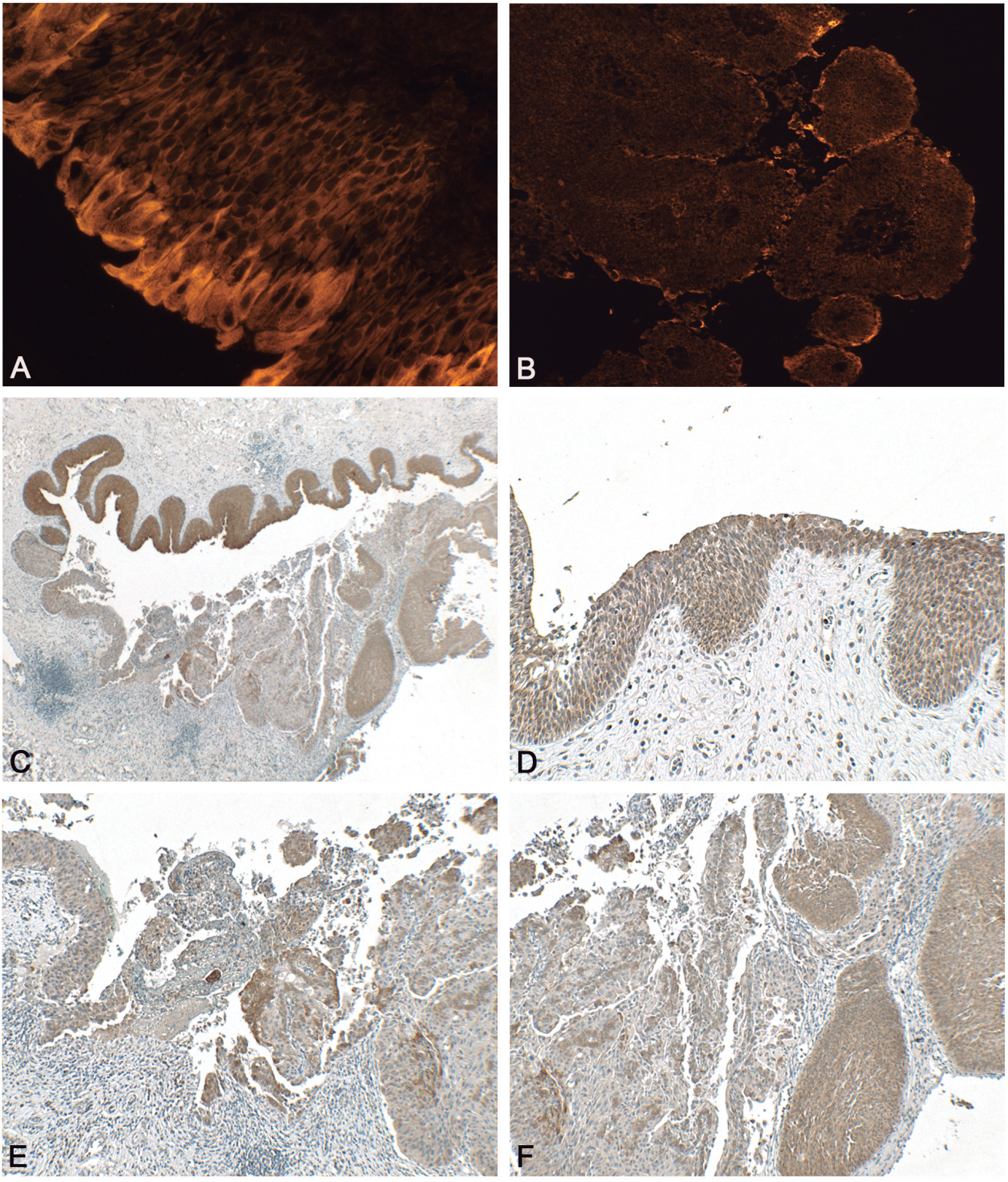

Fig. 3. Immunofluorescence and immunohistochemistry for ACSL5. **A.** Enriched staining of Cy3-anti-ACSL5 in superficial cell layers of normal urothelium. **B.** Moderate Cy3-anti-ACSL5 expression in a well differentiated papillary tumour. **C-F.** DAB-developed anti-ACSL5 immunohistochemistry of normal urothelium, carcinoma in situ (CIS) and invasive carcinoma. **C.** Overview. **D.** Normal urothelium. **E.** Left side: CIS, right side: invasive carcinoma. **F.** Left side: invasive carcinoma poorly differentiated, right side: invasive carcinoma well differentiated. A, D, E, F, x 200; B, x 100; C, x 40

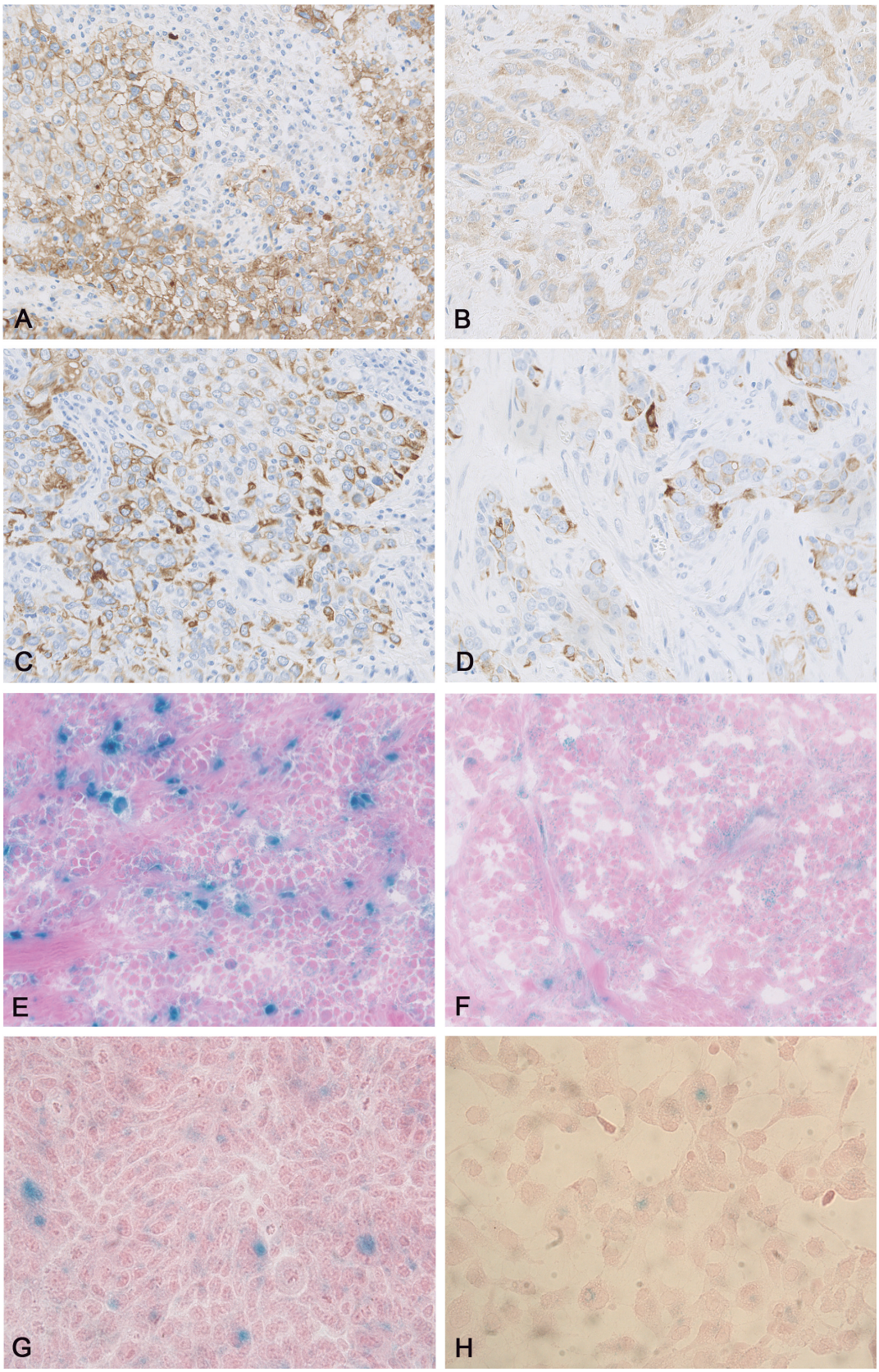

Fig. 4. Immunohistochemistry and Senescence-associated-ß-galactosidase enzymhistochemistry. Left column **A, C, E.** Representative images of ACSL5 upregulated tumour tissue. Right column: **B, D, F.** Representative images of ACSL5 downregulated tumour tissue. **A and B.** Uroplakin III staining. **C and D.** Cytokeratin 20 staining. **E and F.** Senescence-associated-α-galactosidase (sa-ß-gal) enzymehistochemistry. **G and H.** Senescence-associated-ß-galactosidase enzymehistochemistry of cell lines. **G.** RT4 cells with highest levels of ACSL5 expression and **H.** J82 cells with low ACSL5 expression. A-F, x 200; G, H, x 400

most abundant isoform in normal (13.3 fold increase) and tumour bladder tissue (7.3 fold increase). In contrast, ACSL isoform 1 had the lowest abundance in urothelial tissue (1.0 normal urothelium (NU), 0.9 tumour (TU)), followed by ACSL4 (1.5 NU, 0.9 TU). Taking together all patients, an overall differential expression between normal and cancer tissue was found significant for ACSL3 ($p=0.001$), but not ACSL5 ($p=0.095$), probably due to higher standard deviations. Analysis of ACSL5 mRNA-expression with regards to tumour growth pattern (papillary-invasive or solid) or aberrant differentiation (partial squamous differentiation) did not show significant differences (Fig. 2B). However, more detailed pairwise analysis (patient matched normal urothelium and invasive tumour tissue in single comparisons) of ACSL expression revealed highest rates of significant up- or downregulations ($p<0.05$) for ACSL5 expression (88.89% (16/18) significant up- or downregulations) (Table 2). Considering all ACSL isoforms, a downregulation in tumours was evident for isoforms 3, 4 and 5 (significant downregulation: ACSL3 44.4% (8/18), ACSL4 44.4% (8/18) and ACSL5 61.1% (11/18)), whereas less downregulation was detected for ACSL1 (27.8% (5/18)).

Downregulation of ACSL5 expression in tumour tissue compared to patient matched normal urothelium was confirmed by western blot analysis (Fig. 2C). However, for identification of cellular localization immunofluorescence staining and immunohistochemistry for ACSL5 was performed. In normal urothelium, ACSL5 was detected cyto-plasmatically in all urothelial cell layers, with strongest abundance in superficial cells ("umbrella cells") (Fig. 3A). Additional staining of well differentiated non-invasive papillary

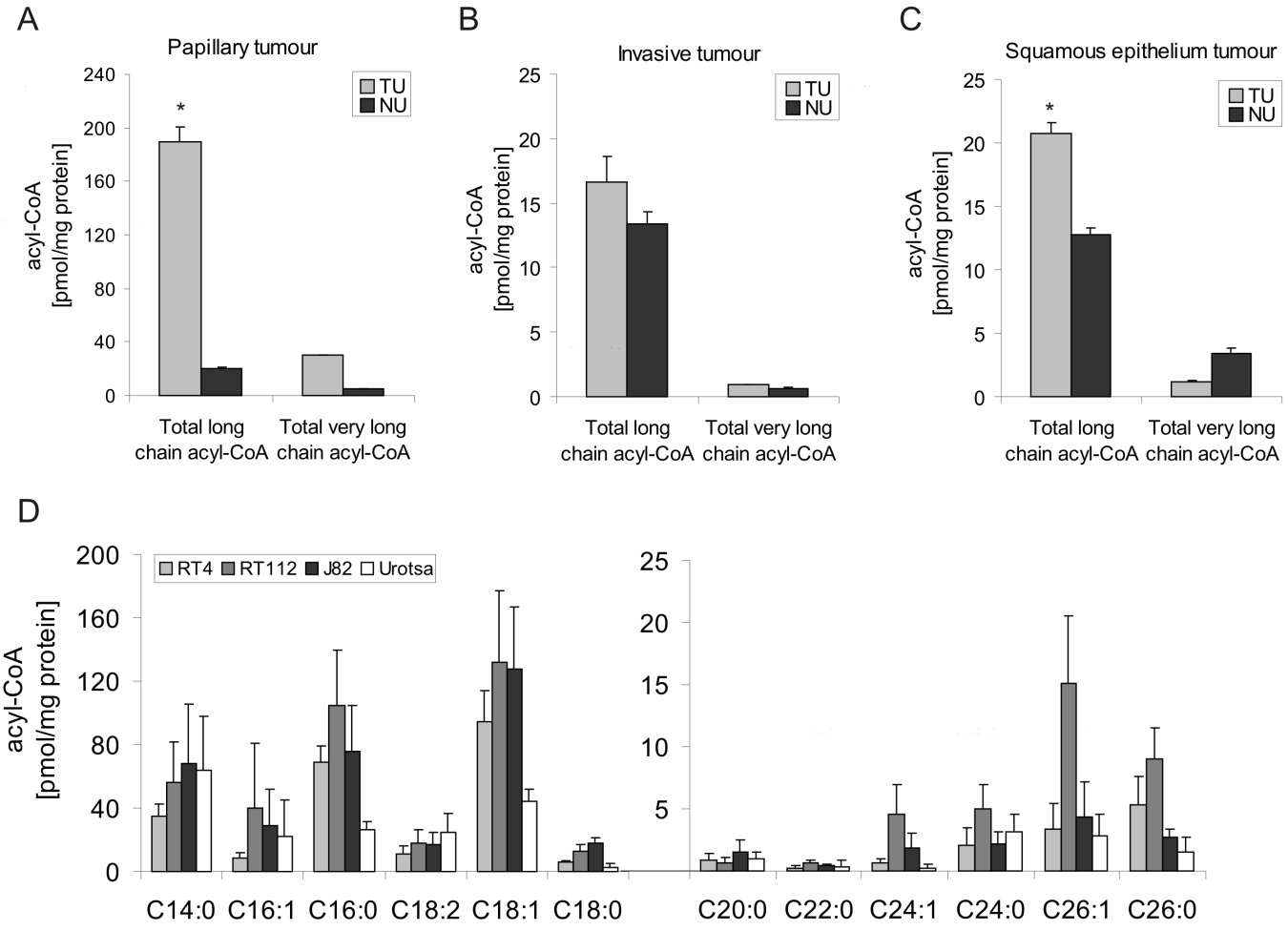

Fig. 5. Acyl-CoA species were extracted from urothelial tissues and cell lines by chloroform/methanol extraction and quantified by LC-MS/MS analysis. **A-C.** Levels of long chain (C14:0 - C20:0) and very long chain (C22:0 - C26:0) acyl-CoA species in malignant versus normal urothelial tissues, analyzed in 3 different types of bladder cancer (n=3, *p<0.05). **D.** Levels of acyl-CoA species dependent on chain length and saturation in urothelial cell lines, RT4, RT112, J82 and Urotsa.

tumours (pTa low grade (G1-2)) revealed slightly reduced staining, mostly due to loss of superficial cells (Fig. 3B). DAB-developed staining of transversal sections including normal urothelium, carcinoma in situ and invasive carcinoma showed highest expression of ACSL5 protein in normal urothelium (Fig. 3C,D). Subsequent gradual loss was observed in carcinoma in situ (Fig. 3C,E left half) or well differentiated invasive carcinoma (Fig. 3F right half) and weak expression in less differentiated invasive carcinoma (Fig. 3E,F left half).

Expression of ACSL5 in bladder cancer correlates with differentiation and senescence markers

ACSL5-mRNA upregulated and downregulated tumour samples (each n=4), as well as corresponding normal urothelium were chosen for further immuno-histochemical analysis and senescence-associated-ß-galactosidase enzymehistochemistry. Uroplakin III, a marker of terminal differentiation in urothelium, was significantly (p=0.015) associated with ACSL5 upregulation (Fig. 4A,B). Cytokeratin 20 showed the same trend but was statistically not significant (p=0.174) (Fig. 4C,D). Possibly senescence associated molecules p16INK4A and p53 resulted in variable staining intensities in both ACSL5 up- and downregulated tumours, without any significant correlation (p=0.067 and p=0.353). These results may be distorted, as both molecules are not selectively involved in senescence, and both TP53 mutations and impairment of p16 are quite frequent events in bladder cancer. Stainings of cell lines did not provide consistent results (i.e. Urotsa negative for Cytokeratin 20 and Uroplakin III, but positive for p16INK4A) and therefore have not been considered. Senescence-associated-ß-galactosidase activity was significantly associated with ACSL5 upregulation in tumours (p=0.03) (Fig. 4E,F) and highest activity was also found in RT4 cells. RT112 and Urotsa showed no ß-galactosidase activity, and in J82 enzyme activity was minimal (Fig. 4G,H).

Acyl-CoA synthesis is upregulated in urothelial tumours

Based on the gradual loss of ACSL isoforms in tumour tissues and cell lines we hypothesized that acyl-CoA levels, the products of ACSLs, were diminished with decreasing cellular differentiation in urothelial cancers. Surprisingly, acyl-CoA synthesis was increased in tumour tissues (Fig. 5A-C). LC-MS/MS showed that the decrease of ACSL expression had no direct influence on acyl-CoA levels. Despite the diversity of the analyzed cell lines and tumour types, the data were unanimous, revealing a strong upregulation of acyl-CoA in cancerous tissues. Particularly in the papillary-invasive tumour phenotype, acyl-CoA levels were 6-8-fold enhanced compared to normal urothelium (Fig. 5A). To determine whether the chain length and saturation of acyl-CoA had an impact on tumour grade and cell differentiation, we investigated the levels of different acyl-CoA subspecies in urothelial cell lines. Mass spectrometry showed the highest acyl-CoA levels in cell line RT112, a model for papillary-invasive bladder cancer with moderate differentiation (still low grade according to 2004 WHO/ISUP classification). When comparing acyl-CoA synthesis of RT 112 with RT4, a cell line derived from a well-differentiated tumour (low grade), most acyl-CoA species were slightly downregulated in relation to the differentiation grade. J82, a cell line derived from a solid invasive tumour with poor differentiation (high grade), revealed a chain length specific upregulation of acyl-CoA species, C14:0 and C18:0, correlating with the histological dedifferentiation. Compared to Urotsa, a normal urothelium cell line, all cancer cell lines showed a strong upregulation of most acyl-CoA species, especially C16:0, C18:1, C18:0, C24:1, C26:1, C26:0. In summary, LC-MS/MS demonstrated a positive correlation between tumour grade and acyl-CoA synthesis for most species and a chain-length dependent correlation between histological dedifferentiation and acyl-CoA levels.

Discussion

This study describes for the first time an expression of ACSLs, and especially ACSL5, in human bladder tissue. ACSLs are expressed in several tissues; isoform 5 is mainly expressed in tissues with high (intestine, skin) or cyclic (endometrium) turnover (Gassler et al., 2003, 2005a,b; Gaisa et al., 2008), presumably due to its central role in lipid biosynthesis. Complex lipids minister to cellular membrane formation (Sumper and Träuble, 1973) during cell propagation and replacement. The urothelium is an epithelium with slow turnover rates and long-lived cells (more than 200 days, Cooper, 1972; Hicks, 1975), thus not predominantly a candidate for high ACSL5 expression. However, the histological architecture of normal urothelium with superficial ("umbrella") cells containing the highly specialized asymmetric unit membrane (AUM) structure (plaque) on the cell surface for sealing and robustness purpose, supposes enriched lipid levels. Indeed, investigations regarding subcellular distribution of free fatty acids and phospholipids as well as endogenous lipase activity in rabbit bladder tissue showed highest concentrations of each component in the mucosa and in mitochondrial fractions (O'Connor et al., 1999). Further analysis of rat transitional epithelium showed a differential plasma membrane lipid composition and the presence of a specific fatty acid (20:3n-9), possibly reflecting the unique morphology and characteristic fatty acid metabolism of this specialized epithelium (Calderon et al., 1998). Consistent with these findings we found ACSL5 expression in all urothelial cell layers with an enriched protein synthesis in superficial cell layers. In papillary or flat/invasive tumours the anti-ACSL5 immunostainings were decreased. This could be in part due to a simple loss of terminally differentiated umbrella

cells during tumour development, but it is also known that several proteins/enzymes show altered levels in malignant conditions, possibly due to changes in metabolic requirements or pathway alterations.

Little is known about the metabolic status of normal and malignant human bladder epithelium. Nevertheless, several studies in animals on dietary fat exposure and their effects on urothelium revealed altered lipid profiles and changes in uroplakin properties of the rodent urothelial plasma membrane (Bongiovanni et al., 2005) and modulations of acrylamide-induced preneoplastic urothelial proliferation or apoptosis depending on the type of fatty acids (Cremonezzi et al., 2001, 2004; Zhang et al., 2010). Additionally, more recent mass spectrometry work on canine transitional cell carcinoma tissue and adjacent normal urothelium showed increased levels of certain glycerophospholipids and free fatty acids in tumour tissues, but also in a lower number of cases in normal tissue (Dill et al., 2009). Our LC-MS/MS data revealed an upregulation of acyl-CoA levels in human urothelial tumour tissues compared to normal urothelia, thus, confirming the hypothesis that alterations in the lipidomic status of normal and malignant human bladder epithelium are present and play an important role in the pathogenesis of bladder cancer. Although we anticipated a decrease of acyl-CoA synthesis -because of ACSL downregulation-, our results show an acyl-CoA increase. This increase could potentially be induced by other acyl-CoA synthesizing enzymes like fatty acid transport proteins (FATPs) which are known to not only transport acyl-CoAs but also catalyze their synthesis. FATPs have not been analyzed in urothelial tissues so far, but their expression pattern might explain high acyl-CoA synthesis in malignant tissues. These results prove that changes in the metabolic status exist, and possibly could attenuate or enforce the microenvironment according to a modifier concept. So far, marginal changes on cellular levels and increased risk of bladder cancer due to dietary effects/metabolic changes are assumed, but the links between high fatty intake, aberrant levels of metabolizing enzymes/carrier proteins and the mechanisms by which these protein alterations contribute to cancer development have not been fully elucidated. Only a few reports on involvement of enzymes of the fatty acid metabolism in bladder cancer exist. Philips et al. have shown that the expression of 15-lipoxygenase-1 (15-LO-1), a polyunsaturated fatty acid (PUFA)-metabolizing enzyme, varied with bladder cancer progression (Philips et al., 2008). In advanced tumour stages (T3/T4) a statistically significant decrease in 15-LO-1 expression in comparison to normal tissue was found. Much earlier, Celis et al. found in 2D-gel studies on bladder tumours a loss of a fatty acid binding protein with homology to the adipocyte isoform (A-FABP) during various stages of tumour progression (low grade tumours to stage III and IV neoplasms) (Celis et al., 1996). These proteins may play a role in intracellular lipid transport and metabolism, but there is also evidence that long-chain fatty acids and their metabolites participate as primary or secondary messengers in specific signaling pathways (Glatz et al., 1995). Our workgroup was able tocould provide substantial evidence for an involvement of ACSL5 in hepatocellular apoptosis (Reinartz et al., 2010). Over-expression of ACSL5 decreased hepatocellular viability and increased susceptibility to TRAIL and TNF·ß whereas knockdown of ACSL5 reduced apoptosis susceptibility. Using lipidomic mass spectrometry we found that ACSL5 has a profound effect on the partitioning of acyl-CoAs to sphingolipids. Sphingolipids, a subgroup of lipids with a sphinganine backbone, are important regulators of cell death and survival (Zheng et al., 2006). High ACSL5 activity enhanced synthesis of long-chain acyl-CoA by 50%. Ceramide as well as sphingomyeline levels were increased 2-3-fold. Thus, it becomes apparent, that alterations in sphingolipid metabolism contribute to ACSL5-mediated apoptotic effects. A modulation of signaling pathways responsible for cell differentiation, proliferation, apoptosis or senescence can have substantial effects for induction of tumour formation or progression and further work has to be done to investigate the mechanisms by which ACSLs and their metabolic products interfere with pathways contributing to bladder tumour formation and progress. If these pathway alterations could be identified, a development of possible new drug targets would be possible. Either a different blocking or activation mechanism of the pathway itself or specific supplements or stabilizers for enzymes could prevent the aberrant signaling and suppress tumour formation or progression. Attempting to re-balance the metabolomic equilibrium of the urothelium offers a further opportunity of tumour treatments and prevention and marks a significant field of future drug therapy in bladder cancer.

Acknowledgements. The authors are grateful for the excellent technical support provided by Kerstin Ertmer, Kerstin Raupach, Ute Weusten and Cordelia Geisler. This study was supported by the german Research Foundation (DFG) grant GA 785/6-1 and Deutsche Krebshilfe grant 109313.

References

Bongiovanni G.A., Eynard A.R. and Calderón R.O. (2005). Altered lipid profile and changes in uroplakin properties of rat urothelial plasma membrane with diets of different lipid composition. Mol. Cell. Biochem. 271, 69-75.

Calderon R.O., Glocker M. and Eynard A.R. (1998). Lipid and fatty acid composition of different fractions from rat urinary transitional epithelium. Lipids 33, 1017-1022.

Celis J.E., Ostergaard M., Basse B., Celis A., Lauridsen J.B., Ratz G.P., Andersen I., Hein B., Wolf H., Orntoft T.F. and Rasmussen H.H. (1996). Loss of adipocyte-type fatty acid binding protein and other protein biomarkers is associated with progression of human bladder transitional cell carcinomas. Cancer Res. 56, 4782-4790.

Chomczynski P. (1993). A reagent for the single-step simultaneous

isolation of RNA, DNA and proteins from cell and tissue samples. Biotechniques 15, 532-534, 536-537.

Cooper E.H. (1972). The biology of bladder cancer. Ann. R. Coll. Surg. Engl. 51, 1-16.

Cremonezzi D.C., Silva R.A., del Pilar Díaz M., Valentich M.A. and Eynard A.R. (2001). Dietary polyunsatured fatty acids (PUFA) differentially modulate melamine-induced preneoplastic urothelial proliferation and apoptosis in mice. Prostaglandins Leukot. Essent. Fatty Acids. 64, 151-159.

Cremonezzi D.C., Díaz M.P., Valentich M.A. and Eynard A.R. (2004). Neoplastic and preneoplastic lesions induced by melamine in rat urothelium are modulated by dietary polyunsaturated fatty acids. Food Chem. Toxicol. 42, 1999-2007.

Dill A.L., Ifa D.R., Manicke N.E., Costa A.B., Ramos-Vara J.A., Knapp D.W. and Cooks R.G. (2009). Lipid profiles of canine invasive transitional cell carcinoma of the urinary bladder and adjacent normal tissue by desorption electrospray ionization imaging mass spectrometry. Anal. Chem. 81, 8758-8764.

Faergeman N.J. and Knudsen J. (1997). Role of long-chain fatty acyl-CoA esters in the regulation of metabolism and in cell signalling. Biochem. J. 323, 1-12.

Ferlay J., Shin H.R., Bray F., Forman D., Mathers C. and Parkin D.M. (2010). Estimates of worldwide burden of cancer in 2008: GLOBOCAN 2008. Int. J. Cancer. 127, 2893-2917.

Fink L., Seeger W., Ermert L., Hänze J. Stahl U. Grimminger F., Kummer W. and Bohle R.M. (1998) Real-time quantitative RT-PCR after laser-assisted cell picking. Nat Med 4, 1329-1333.

Gaisa N.T., Köster J., Reinartz A., Ertmer K., Ehling J., Raupach K., Perez-Bouza A., Knüchel R. and Gassler N. (2008). Expression of acyl-CoA synthetase 5 in human epidermis. Histol. Histopathol. 23, 451-458.

Gassler N., Schneider A., Kopitz J., Schnölzer M., Obermüller N., Kartenbeck J., Otto H.F. and Autschbach F. (2003). Impaired expression of acyl-CoA-synthetase 5 in epithelial tumors of the small intestine. Hum. Pathol. 34, 1048-1052.

Gassler N., Kopitz J., Tehrani A., Ottenwälder B., Schnölzer M., Kartenbeck J., Lyer S., Autschbach F., Poustka A., Otto H.F. and Mollenhauer J. (2004). Expression of acyl-CoA synthetase 5 reflects the state of villus architecture in human small intestine. J. Pathol. 202, 188-196.

Gassler N., Herr I., Schneider A., Penzel R., Langbein L., Schirmacher P. and Kopitz J. (2005a). Impaired expression of acyl-CoA synthetase 5 in sporadic colorectal adenocarcinomas. J. Pathol. 207, 295-300.

Gassler N., Yang S.H., Keith M., Helmke B.M., Schirmacher P. and Obermüller N. (2005b). Expression of acyl-CoA synthetase 5 in human endometrium and in endometrioid adenocarcinomas. Histopathology 47, 501-507.

Gassler N., Roth W., Funke B., Schneider A., Herzog F., Tischendorf J.J., Grund K., Penzel R., Bravo I.G., Mariadason J., Ehemann V., Sykora J., Haas T.L., Walczak H., Ganten T., Zentgraf H., Erb P., Alonso A., Autschbach F., Schirmacher P., Knüchel R. and Kopitz J. (2007). Regulation of enterocyte apoptosis by acyl-CoA synthetase 5 splicing. Gastroenterology 133, 587-598.

Glatz J.F., Börchers T., Spener F. and van-der-Vusse G.J. (1995). Fatty acids in cell signalling: modulation by lipid binding proteins. Prostaglandins Leukot. Essent. Fatty Acids. 52, 121-127.

Haynes C.A., Allegood J.C., Sims K., Wang E.W., Sullards M.C. and Merrill A.H. (2008). Quantitation of fatty acyl-coenzyme As in mammalian cells by liquid chromatography-electrospray ionization tandem mass spectrometry. J. Lipid Res. 49, 1113-1125.

Hicks R.M. (1975). The mammalian urinary bladder: an accommodating organ. Biol. Rev. Camb. Philos. Soc. 50, 215-246.

Hong Y.M. and Loughlin K.R. (2008). Economic impact of tumor markers in bladder cancer surveillance. Urology 71, 131-135.

Howlader N., Noone A.M., Krapcho M., Neyman N., Aminou R., Waldron W., Altekruse S.F., Kosary C.L., Ruhl J., Tatalovich Z., Cho H., Mariotto A., Eisner M.P., Lewis D.R., Chen H.S., Feuer E.J., Cronin K.A. and Edwards B.K. (2011). SEER Cancer Statistics Review, 1975-2008, National Cancer Institute. Bethesda, MD, http://seer.cancer.gov/csr/1975_2008/, based on November 2010 SEER data submission, posted to the SEER web site.

Lopez-Beltran A., Sauter G., Gasser T., Hartmann A., Schmitz-Dräger B.J., Helpap B., Ayala A.G., Tamboli P., Knowles M.A., Sidransky D., Cordon-Cardo C., Jones P.A., Cairns P., Simon R., Amin M.B. and Tyczynski J.E. (2004). Tumours of the urinary system. In: World Health Organization Classification of Tumours. Pathology and genetics of tumours of the urinary system and male genital organs. Eble J.N., Sauter G., Epstein J.I. and Sesterhenn I.A. (eds). IARC Press. Lyon. France pp 89-158.

Mashek D.G., Bornfeldt K.E., Coleman R.A., Berger J., Bernlohr D.A., Black P., DiRusso C.C., Farber S.A., Guo W., Hashimoto N., Khodiyar V., Kuypers F.A., Maltais L.J., Nebert D.W., Renieri A., Schaffer J.E., Stahl A., Watkins P.A., Vasiliou V. and Yamamoto T.T. (2004). Revised nomenclature for the mammalian long-chain acyl-CoA synthetase gene family. J. Lipid. Res. 45, 1958-1961.

Masters J.R., Hepburn P.J., Walker L., Highman W.J., Trejdosiewicz L.K., Povey S., Parkar M., Hill B.T., Riddle P.R. and Franks L.M. (1986). Tissue culture model of transitional cell carcinoma: characterization of twenty-two human urothelial cell lines. Cancer Res. 46, 3630-3636.

Mostofi F.K., Sobin L.H. and Torloni H. (1973). International histological classification of tumours No. 10 Histological typing of urinary bladder tumours. World Health Organization. Geneva. pp 15-36.

O'Connor L.J., Nicholas T. and Levin R.M. (1999). Subcellular distribution of free fatty acids, phospholipids, and endogenous lipase activity of rabbit urinary bladder smooth muscle and mucosa. Adv. Exp. Med. Biol. 462, 265-273.

Pfaffl M.W. (2001). A new mathematical model for relative quantification in real-time RT-PCR. Nucleic Acids Res. 29, e45.

Pfaffl M.W., Horgan G.W. and Dempfle L. (2002). Relative expression software tool (REST©) for group-wise comparison and statistical analysis of relative expression results in real-time PCR. Nucleic Acids Res. 30, e36.

Philips B.J., Dhir R., Hutzley J., Sen M. and Kelavkar U.P. (2008). Polyunsaturated fatty acid metabolizing 15-Lipoxygenase-1 (15-LO-1) expression in normal and tumorigenic human bladder tissues. Appl. Immunohistochem. Mol. Morphol. 16, 159-164.

Reinartz A., Ehling J., Leue A., Liedtke C., Schneider U., Kopitz J., Weiss T., Hellerbrand C., Weiskirchen R., Knüchel R. and Gassler N. (2010). Lipid-induced up-regulation of human acyl-CoA synthetase 5 promotes hepatocellular apoptosis. Biochim. Biophys. Acta 1801, 1025-1035.

Remmele W. and Stegner H.E. (1987). Recommendation for uniform definition of an immunoreactive score (IRS) for immunohistochemical estrogen receptor detection (ER-ICA) in breast cancer tissue. Pathologe 8, 138-140.

Rigby C.C. and Franks L.M. (1970). A human tissue culture cell line

from a transitional cell tumour of the urinary bladder: growth, chromosome pattern and ultrastructure. Br. J. Cancer 24, 746-754.

Rossi M.R., Masters J.R., Park S., Todd J.H., Garrett S.H., Sens M.A., Somji S., Nath J. and Sens D.A. (2001). The immortalized UROtsa cell line as a potential cell culture model of human urothelium. Environ. Health. Perspect. 109, 801-808.

Soupene E. and Kuypers F.A. (2008). Mammalian long-chain acyl-CoA synthetases. Exp. Biol. Med. 233, 507-521.

Sumper M. and Träuble H. (1973). Membranes as acceptors for palmitoyl CoA in fatty acid biosynthesis. FEBS Lett. 30, 29-34.

Yamashita Y., Kumabe T., Cho Y.Y., Watanabe M., Kawagishi J., Yoshimoto T., Fujino T., Kang M.J. and Yamamoto T.T. (2000). Fatty acid induced glioma cell growth is mediated by the acyl-CoA synthetase 5 gene located on chromosome 10q25.1-q25.2, a region frequently deleted in malignant gliomas. Oncogene 19, 5919-5925.

Wu X.R. (2005). Urothelial tumorigenesis: a tale of divergent pathways. Nat. Rev. Cancer 5, 713-725.

Zhang X., Zhao C. and Jie B. (2010). Various dietary polyunsaturated fatty acids modulate acrylamide-induced preneoplastic urothelial proliferation and apoptosis in mice. Exp. Toxicol. Pathol. 62, 9-16.

Zheng W., Kollmeyer J., Symolon H., Momin A., Munter E., Wang E., Kelly S., Allegood J.C., Liu Y., Peng Q., Ramaraju H., Sullards M.C., Cabot M. and Merrill A.H. Jr (2006). Ceramides and other bioactive sphingolipid backbones in health and disease: Lipidomic analysis, metabolism and roles in membrane structure, dynamics, signaling and autophagy. Biochim. Biophys. Acta 1758, 1864-1884.

Accepted October 16, 2012